Spectrochimica Acta Part A 75 (2010) 753–759

Contents lists available at ScienceDirect

Spectrochimica Acta Part A: Molecular and Biomolecular Spectroscopy

journal homepage: www.elsevier.com/locate/saa

# Synthesis, characterization and spectroscopic investigation of a novel phenylhydrazone Schiff base with solvatochromism

Mingtian Li[a,*], Jun Huang[b], Xuan Zhou[b], Hong Luo[a]

[a] *Institute of Materials and Chemical Engineering, Sichuan University of Science and Engineering, Zigong 643000, China*
[b] *Key Laboratory of Fiber Optic Sensing Technology and Information Processing (Ministry of Education), Wuhan University of Technology, Wuhan 430070, China*

ARTICLE INFO

*Article history:*
Received 13 August 2009
Accepted 20 November 2009

*Keywords:*
Phenylhydrazone
Crystal structure
Thermochromism
Solvatochromism
Mechanism

ABSTRACT

A novel Schiff base of 4,5-diazafluorene-9-*p*-nitrophenylhydrazone (DAFND) has been synthesized and characterized. The crystal structures of DAFND and its analogue 4,5-diazafluorene-9-phenylhydrazone (DAFPD) were determined by single crystal X-ray diffraction method. X-ray analyses reveal that DAFPD comprise of a nonplanar molecule and all atoms of DAFND are essentially coplanar. The color of DAFND changes from brown to blue when heated, so called thermochromism and the spectroscopic properties of the two compounds are investigated by electronic absorption spectra, showing DAFND possess solvatochromism, while DAFPD does not have thermochromic and solvatochromic properties. The $\lambda_{max}$ of DAFND within various pure solvents are different ranging from 370 nm in toluene to 614 nm in pyridine. The imaginable mechanisms of thermochromism and solvatochromism are proposed.

## 1. Introduction

Hydrazones and their metal complexes are of current interest for their physico-chemical properties and applications in many fields such as sensors, non-linear optics, medicine, DNA probe and others [1–8], which is determined by their structures influenced largely by the type and position of the substituent group. As far as we know, however, the derivatives of phenylhydrazone without hydroxy hardly have thermochromism or solvatochromism. The compounds exhibit the change of color reversibly or irreversibly with temperature variation, so called thermochromism [9,10], and the term "solvatochromism" describes a significant change in position or intensity of an absorption or emission band of a compound in solution, when the polarity of the medium is changed [11]. The thermochromic compounds are much interesting in various applications such as smart dyes, temperature sensitive light filters, fiber optic biosensors and imaging systems as well [9,12,13], while solvatochromic dyes play a key role in the understanding of solvent polarity effects and are increasingly important as probes of complex biological systems [14–16]. As far as we are concerned, the Schiff bases of phenylhydrazone without hydroxy hardly have thermochromism and solvatochromism. In this study, we found for the first time that 4,5-diazafluorene-9-*p*-nitrophenylhydrazone (DAFND) hold thermochromic and solvatochromic properties, demonstrating the notable originality of the research.

DAFPD was first reported by Mlochowski and Szulc in 1983 [17], however, its crystal structure has not yet been reported. In order to interpret the property difference from structure, the crystal structures of two Schiff bases are presented in this paper. Their spectroscopic properties have been explored by electronic absorption spectra and the mechanisms on thermochromism and solvatochromism of DAFND are proposed based on the structural difference of the two compounds.

## 2. Experimental

### 2.1. Materials

All solvents involving in spectral experiments were of UV grade (Merck UVASOL). All other analytical reagents were obtained from commercial sources and used without further purification. Doubly distilled water was used. 4,5-diazafluorene-9-one was prepared following the literature procedure [18].

### 2.2. Syntheses of DAFPD and DAFND

*DAFPD*: was synthesized according to the literature [17], and the yellow block crystals were obtained from recrystallization with methanol. Yield: 0.261 g, 80%. mp: 225–227 °C. $^1$H NMR (600 MHz, CDCl$_3$, $\delta$): 8.95 (s, 1H), 8.77 (d, $J$ = 4.2 Hz, 1H), 8.70 (d, $J$ = 4.2 Hz, 1H), 8.23 (t, $J$ = 3.6 Hz, 2H), 7.34–7.42 (m, 6H), 7.08 (d, $J$ = 6.0 Hz, 1H). Anal. calcd. for $C_{17}H_{12}N_4$: C, 74.98; H, 4.44; N, 20.58. Found: C, 74.73; H, 4.65; N, 20.87%.

---

* Corresponding author. Tel.: +86 813 5505837; fax: +86 813 5505837.
*E-mail address:* limt63646616@yahoo.com.cn (M. Li).

1386-1425/$ – see front matter. Crown Copyright © 2009 Published by Elsevier B.V. All rights reserved.
doi:10.1016/j.saa.2009.11.050

**Table 1**
Crystallographic data for DAFPD and DAFND.

| Crystal data | DAFPD | DAFND |
|---|---|---|
| Empirical formula | $C_{17}H_{12}N_4$ | $C_{17}H_{11}N_5O_2$ |
| Formula weight | 272.31 | 317.31 |
| Crystal system | Orthorhombic | Monoclinic |
| Space group | *P*2(1)2(1)2(1) | *P*21/*n* |
| $a$ (Å) | 5.4372(10) | 9.063(2) |
| $b$ (Å) | 11.078(2) | 13.473(3) |
| $c$ (Å) | 22.589(4) | 12.215(3) |
| $\beta$ (°) | 90.00 | 104.691(4) |
| $V$ (Å$^3$) | 1360.7(4) | 1442.7(6) |
| Z | 4 | 4 |
| $\mu$ (mm$^{-1}$) | 0.083 | 0.101 |
| $F$(0 0 0) | 568 | 656 |
| $\theta$ Range (°) | 1.80 to 27.49 | 2.29 to 28.00 |
| Index ranges | $-6 \le h \le 6$<br>$-12 \le k \le 14$<br>$-27 \le l \le 28$ | $-11 \le h \le 8$<br>$-17 \le k \le 17$<br>$-15 \le l \le 16$ |
| No. refln./unique | 9589/1812 | 9237/3443 |
| Data/restraints/parameters | 1812/0/194 | 3443/19/214 |
| $S$ on $F^2$ | 1.115 | 1.044 |
| $R_1$, $wR_2$ [$I > 2\sigma(I)$][a,b] | $R_1 = 0.0502$,<br>$wR_2 = 0.1087$ | $R_1 = 0.0608$,<br>$wR_2 = 0.0853$ |
| $R_1$, $wR_2$ (all data)[a,b] | $R_1 = 0.0745$,<br>$wR_2 = 0.1231$ | $R_1 = 0.1298$,<br>$wR_2 = 0.1927$ |
| $\Delta\rho_{min}$ and $\Delta\rho_{max}$ (e/Å$^3$) | 0.214<br>and−0.194 | 0.598<br>and−0.191 |

[a] $R = \sum ||Fo| - |Fc|| / \sum |Fo|$.
[b] $wR = [\sum w(|Fo|^2 - |Fc|^2)^2] / \sum w|Fo|^2]^{1/2}$

*DAFND*: 4–5 drops of acetic acid were added to a methanol solution of 4,5-diazafluorene-9-one (0.182 g, 1.0 mmol) and *p*-nitrophenylhydrazine (0.183 g, 1.2 mmol,). A yellow solid formed after refluxing for 3 h was isolated. Yield: 0.284 g, 90%. mp: 188–189 °C. $^1$H NMR (600 MHz, $CDCl_3$, $\delta$): 9.14 (s, 1H), 8.82 (d, $J = 4.8$ Hz, 1H), 8.75 (d, $J = 4.8$ Hz, 1H), 8.31 (d, $J = 8.4$ Hz, 2H), 8.24 (s, 2H), 7.38–7.44 (m, 4H). Anal. calcd. for $C_{17}H_{11}N_5O_2$: C, 64.35; H, 3.53; N, 22.14. Found: C, 64.67; H, 3.04; N, 22.37%.

### 2.3. Physical measurements

Melting point was measured on Netzsch STA 449 instruments. The temperature ranged from 25 to 184 °C with a speed of 3 °C/min. The electronic absorption spectra were recorded between 200 and 800 nm in a 10 mm path-length cell on a Shimadzu UV-2450 PC spectrophotometer. The UV–vis spectra of thermochromism and solvatochromism were performed with a concentration of $5.0 \times 10^{-4}$ M within various solvents.

### 2.4. X-ray crystallography

X-ray diffraction data for the compounds were collected on a Bruker APEX SMART CCD diffractometer with a graphite-monochromatized Mo Kα radiation ($\lambda = 0.71073$ Å) at 20(2) °C. An empirical absorption correction (SADABS) was applied to the raw intensities [19]. The structures were solved by direct method and refined on $F^2$ by full-matrix least-squares, employing the SHELXTL program [20]. Geometrical calculations and the molecular diagram were obtained with the program PLATON [21]. All non-hydrogen atoms were refined with anisotropic thermal parameters. The H atoms from imine group were located in a different Fourier map and refined with $U_{iso}(H) = 1.5U_{iso}(N)$. H atoms on C atoms were placed in geometrically idealized positions and refined as riding with $U_{iso}(H) = 1.2U_{iso}(C)$. Crystal parameters and details of the data collection and refinement are given in Table 1. Selected bond lengths and angles were listed in Table 2. CCDC: 697125, 685276

## 3. Results and discussion

### 3.1. Crystal structures

Perspective views of DAFPD and DAFND are shown in Figs. 1 and 2. In spite of the different crystal systems, the asymmetric units of the two compounds are the same and contain a neutral molecule. The molecule of DAFPD is absent from nitro group compared with DAFND molecule. X-ray analysis, within DAFND, reveals that the diazafluoren plane forms an angle of 2.83(3)° with the C═N–N plane and the dihedral angle between 4,5-diazafluorenylidene and phenyl planes is 2.58(10)°, which is different from that of the reported compound phenylamine 4,5-diazafluorene-9-one (104.3°) [7], indicating all atoms are essentially coplanar with a r.m.s. deviation of 0.002 Å, and the largest departure is −0.088(3) Å for C2. However, the equivalent angles within DAFPD are 11.6(3)° and 29.15(12)°, respectively, which is obviously larger than those of DAFND, illustrating the planarity of DAFPD is worse than DAFND. Bond lengths and angles of two compounds are in accord with anticipated values [22,23]. The distances of N1–N2 from 4,5-diazafluorenylidene are notably larger than that of the maternal compound 1,10-phenanthroline (phen), and the N–N distances are 3.048(13), 3.0402(13) and 2.623(18) Å for DAFPD, DAFND and phen [24], respectively.

Due to the characteristic conjugated structure, there is significant intermolecular $\pi$–$\pi$ stacking within the two compounds. As for DAFPD, the centroid–centroid distance, $Cg1 \cdots Cg2^{ii}$, between the pyridine rings in two symmetry-related diazafluoren plane is 3.7867(16) Å, [$Cg1$ and $Cg2$ are the centroids of the rings C1–C5/N1 and C6–C10/N2, (ii): $-x+1, y, z$], and the dihedral angle $\alpha$ (between planes $Cg1$ and $Cg2$) and deviation angle $\beta$ (between the $Cg1$–$Cg2$ vector and the normal to centroid $Cg1$) are 2.03° and 24.46°, respectively, indicating there is a significant $\pi$–$\pi$ stacking interaction [25]. Similarly, within DAFND, the centroid–centroid distance between the C6–C10/N2 pyridine ring (centroid $Cg1$) and the C12–C17 ben-

**Table 2**
Selected bond lengths (Å) and angles (°) for DAFPD and DAFND.

| Bond | Dist | Angle | (°) | Angle | (°) |
|---|---|---|---|---|---|
| DAFPD | | | | | |
| C(11)-N(3) | 1.299(3) | C(11)-N(3)-N(4) | 119.3(2) | C(7)-C(11)-N(3)-N(4) | −179.3(2) |
| C(12)-N(4) | 1.407(3) | N(3)-N(4)-C(12) | 120.0(2) | C(4)-C(11)-N(3)-N(4) | −10.4(4) |
| N(3)-N(4) | 1.334(3) | N(3)-C(11)-C(4) | 133.3(3) | C(17)-C(12)-N(4)-N(3) | −3.2(4) |
| N(1)-N(2) | 3.048(13) | C(13)-C(12)-N(4) | 117.9(3) | C(13)-C(12)-N(4)-N(3) | 179.7(3) |
| DAFND | | | | | |
| C(11)-N(3) | 1.307(3) | C(11)-N(3)-N(4) | 120.1(2) | C(7)-C(11)-N(3)-N(4) | 178.3(2) |
| C(12)-N(4) | 1.397(3) | N(3)-N(4)-C(12) | 119.8(2) | C(4)-C(11)-N(3)-N(4) | −2.1(5) |
| N(3)-N(4) | 1.324(3) | N(3)-C(11)-C(4) | 134.9(2) | C(17)-C(12)-N(4)-N(3) | 0.2(4) |
| N(1)-N(2) | 3.0402(13) | C(13)-C(12)-N(4) | 119.2(3) | C(13)-C(12)-N(4)-N(3) | 179.9(2) |

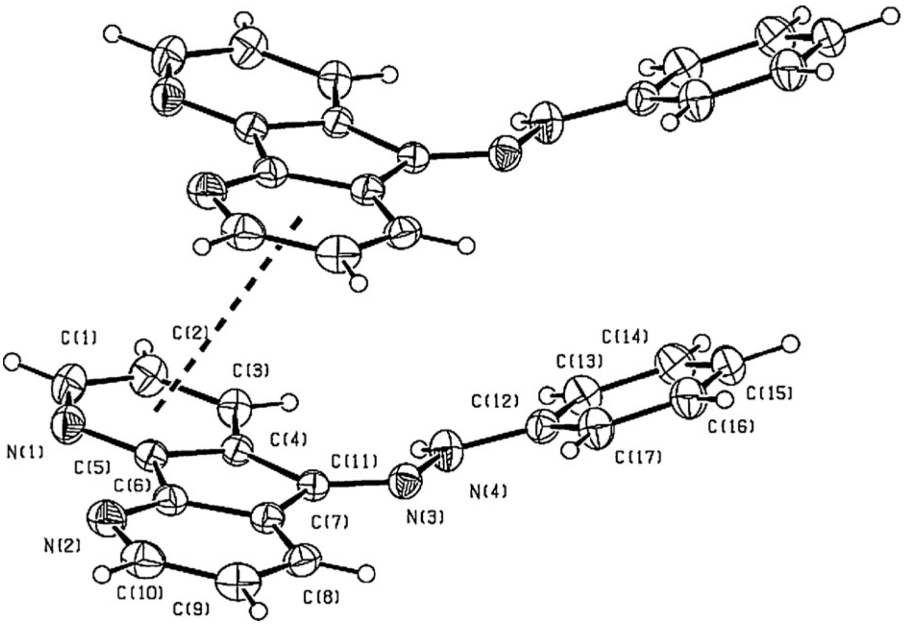

**Fig. 1.** Ortep view of DAFPD.

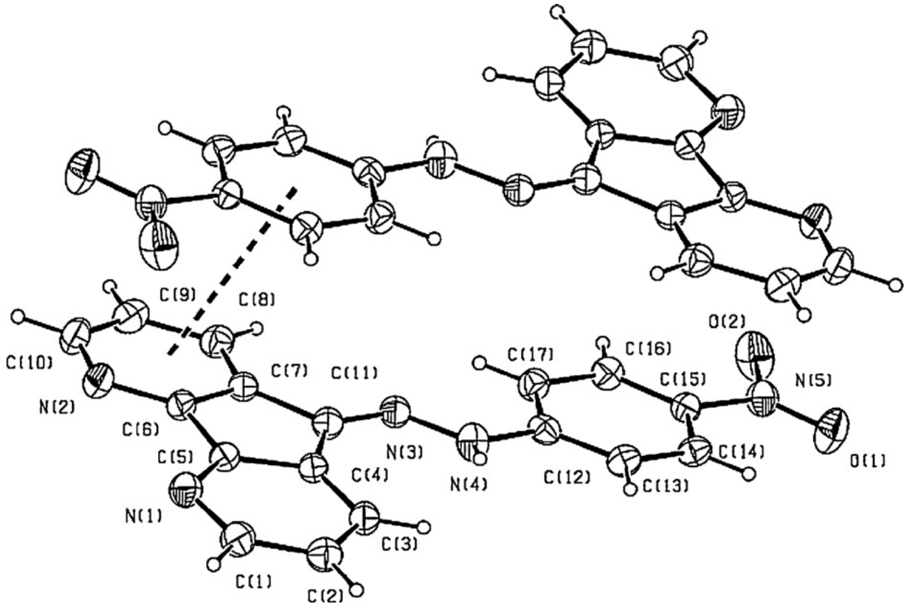

**Fig. 2.** Ortep view of DAFND.

zene ring [$Cg2^{ii}$, (ii): $-x$, $-y$, $-z+1$] is 3.6715(3) Å, while α and $\beta$ are 1.25° and 22.47°, respectively, which indicates that the stacking interaction is stronger than that of DAFPD.

Hydrogen bonds play a key role in the formation of 1D chains and 2D layers and in stabilization of the crystal structures for DAFPD and DAFND, whereas the nitro group is vital to the type of hydrogen bond and the crystal stacking mode. Within DAFPD, the H atom of imine group is linked by a N atom from diazafluoren plane in symmetry-related molecule *via* N···H. N hydrogen bond, and the N atom from a pyridine ring simultaneously links the other H atom of imine group belonging to the third DAFPD molecule, thus 1D zigzag chain along with (0 1 0) direction is formed, as shown in Fig. 3. However, the hydrogen bonds formed by $O_2$ of nitro group and H of imine group within DAFND and the infinite 1D chains are extended along with (0 1 0) direction shown in Fig. 4. The hydrogen bonds as well as the previously discussed $\pi$–$\pi$ stacking interactions

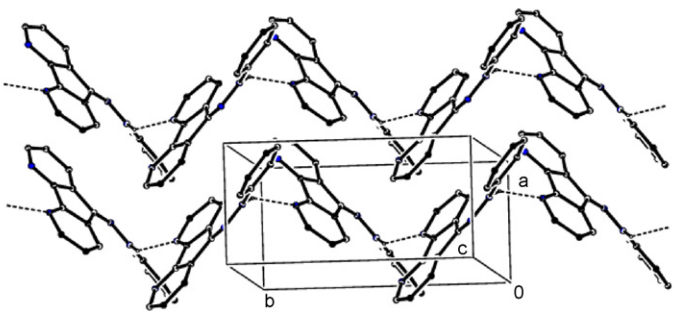

**Fig. 3.** View of packing diagram of DAFPD.

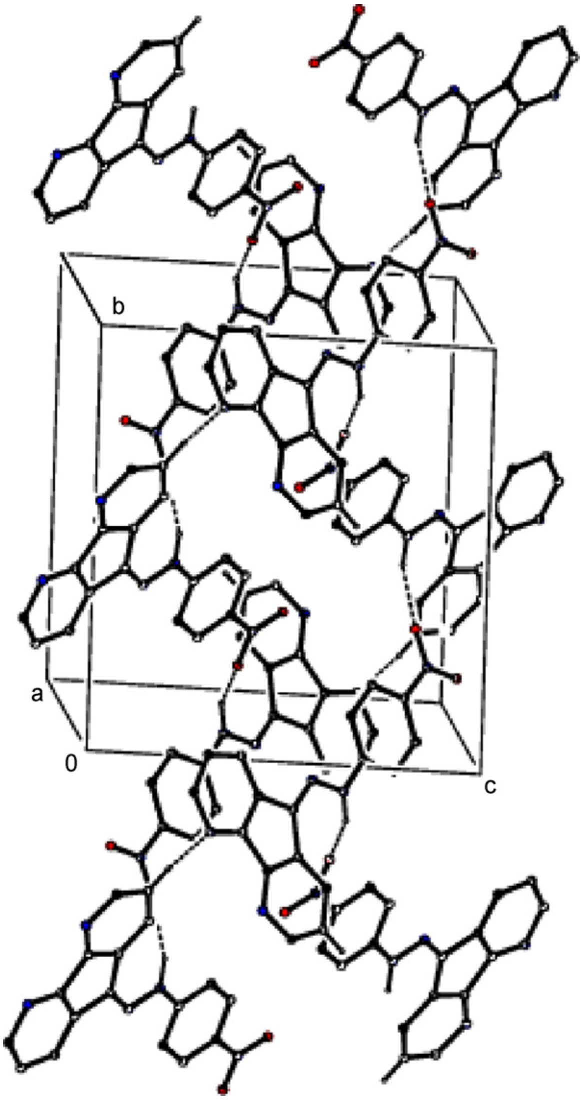

**Fig. 4.** View of packing diagram of DAFND.

take part in the formation of a 2D network and in the stabilization of the crystal structure.

### 3.2. Thermochromism

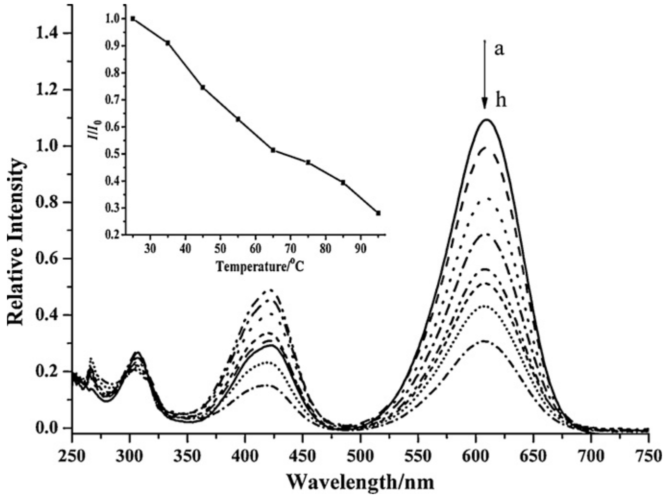

**Fig. 5.** UV–vis spectra of DAFND in DMF at various temperatures.

Table 3 presents the thermal properties of DAFND and DAFPD. The brown color of DAFND at about 95 °C changed to green and then blue in the solid state when heated. The color change is irreversible ranging from 95 to 96 °C. However, DAFPD melt at about 226 °C and had no color change. Obviously, the nitro group is important to thermochromism of DAFND. It is necessary to thermochromism that the planarity and stacking interaction of organic compound [26]. The planarity and stacking interaction of DAFND are better than those of DAFPD (*vide supra*), on the other hand, there may be two isomeric molecular species in DAFND when heated, shown in Scheme 1. The thermochromism of organic compound occurs *via* an equilibrium process between two isomeric molecular species [27]. The conjugated degree of the zwitterionic structure is obviously larger than that of the neutral compound, which is favorable to the electron transfer, so the color changes yellow to green and blue.

As a matter of fact, the tautomerism of DAFND can be proved by the electronic absorption spectra in DMF at various temperatures shown in Fig. 5. The intensities at 609 nm were gradually reduced and had a 30% value of $I_0$ ($T = 25$ °C) at 95 °C, indicating the concentration of DAFND was changed. The imaginable interpretation is that the two isomers take place the structural transformation, which can also be proved the intensities at 423 nm. The intensities were increased in the range of 25 and 75 °C and then obviously decreased to a minimum at 95 °C with little hypochromatic shift from 423 to 418 nm.

### 3.3. Solvatochromism

DAFND exhibits not only thermochromism but also solvatochromism because of the existence of the nitro group. The colors

**Table 3**
Thermal properties of DAFND and DAFPD.

| | mp (°C) | Point of change color | Change color | Acuity | Reversibility |
|---|---|---|---|---|---|
| DAFND | 188–189 | 95–96 | Brown–green–blue | Obvious | Inreversible |
| DAFPD | 225–227 | – | – | – | – |

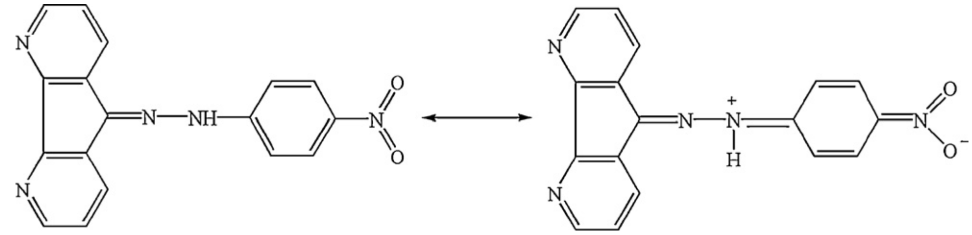

**Scheme 1.** The tautomeric structures of DAFND.

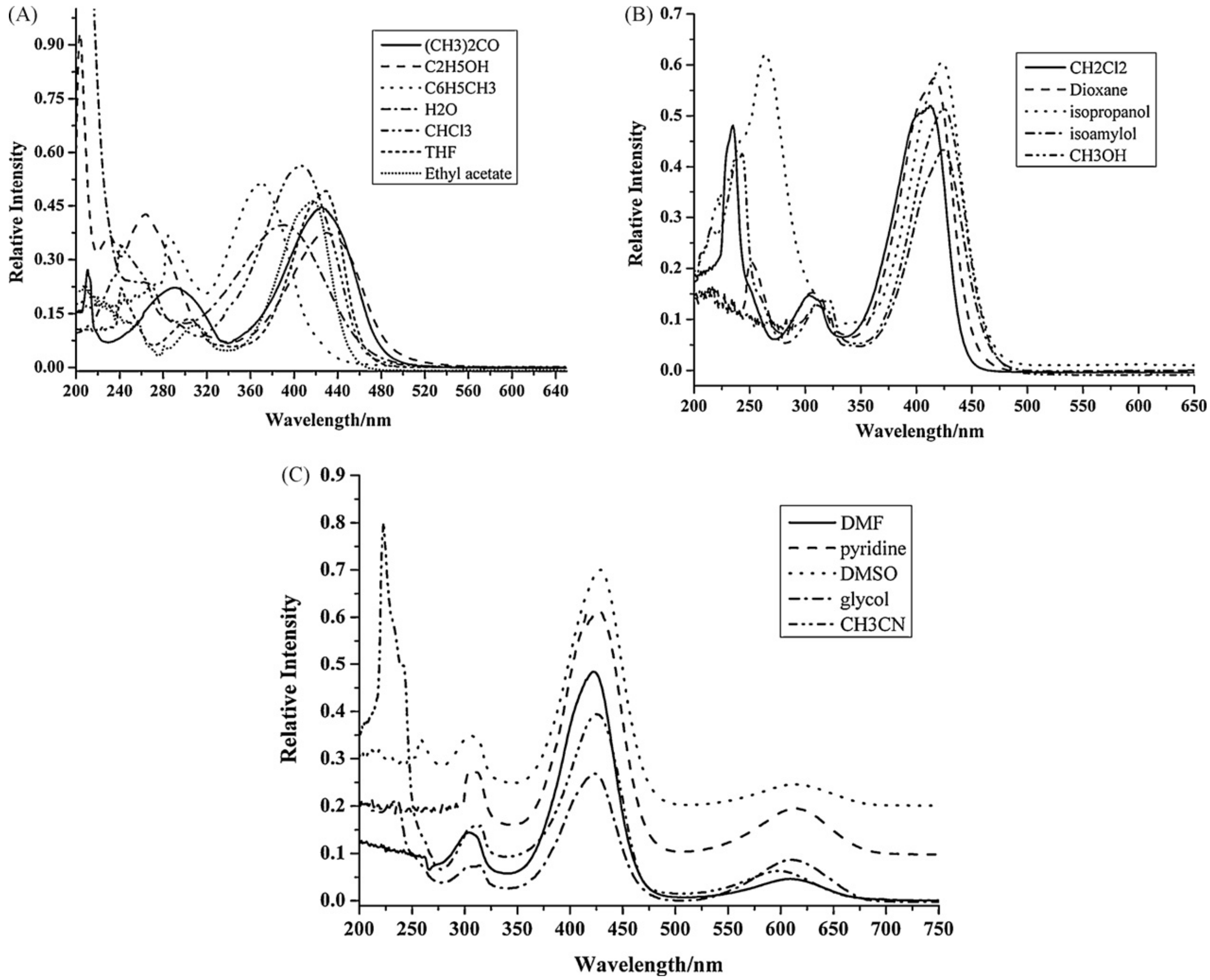

**Fig. 6.** UV–vis spectra of DAFND in various pure solvents.

of DAFND in various pure solvents range from yellow to green and blue, while DAFPD is identical with yellow at the same concentration. The UV–vis spectra of DAFPD and DAFND in different pure solvents were shown in Figs. 6 and 7. The $\lambda_{max}$ of DAFPD in all pure solvents are the same at 395 nm and the intensities are nearly equal.

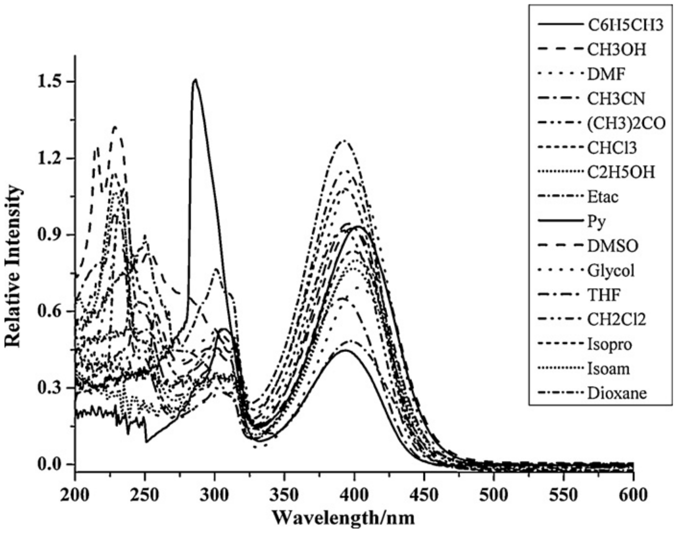

**Fig. 7.** UV–vis spectra of DAFPD in various pure solvents.

However, the positions of the maximal absorption peak for DAFND are different ranging from 370 nm in toluene to 614 nm in pyridine (py) with the diverse intensities. It is interesting that the intensities of DAFND at about 600 nm are smaller than those at about 423 nm in strong polar solvents such as py, DMF, DMSO, acetonitrile and glycol, however, the intensities of the maximal peak at below 430 nm are irregular (Table 4). In the mixed solvents of DMF and methanol, the positions of the maximal peak are red-shift from at 398 nm in methanol to at 609 nm in DMF as the increasing voluminal ratios of DMF, with the intensities raised, as shown in Fig. 8.

Solvatochromic compounds can be described by two extreme resonance contributing structures: one form is quinoidal, nonpolarized, and formally nonaromatic; the other is zwitterionic, polarized, and fully aromatic [11]. The change in the absorption band with solvent arises from variation in the contribution of these canonical forms to the overall resonance hybrid [28]. The nitro group undoubtedly plays a key role in solvatochromism, and the tautomerism is shown Scheme 1.

The solvatochromic behavior can be attributed to a number of specific and nonspecific solute/solvent interactions as summarized in the linear solvation energy relationship (LSER) of Eq. (1) [29]

$$E = E_0 + s\pi * + a\alpha + b\beta \qquad (1)$$

where $s$, $a$, and $b$ are coefficients and $\pi^*$, $\alpha$ and $\beta$ reflect, respectively, the general solvent dipolarity/polarizability, its specific H-bond donating ability, and its specific H-bond accepting ability, which may or may not oppose one another in terms of solvatochromic

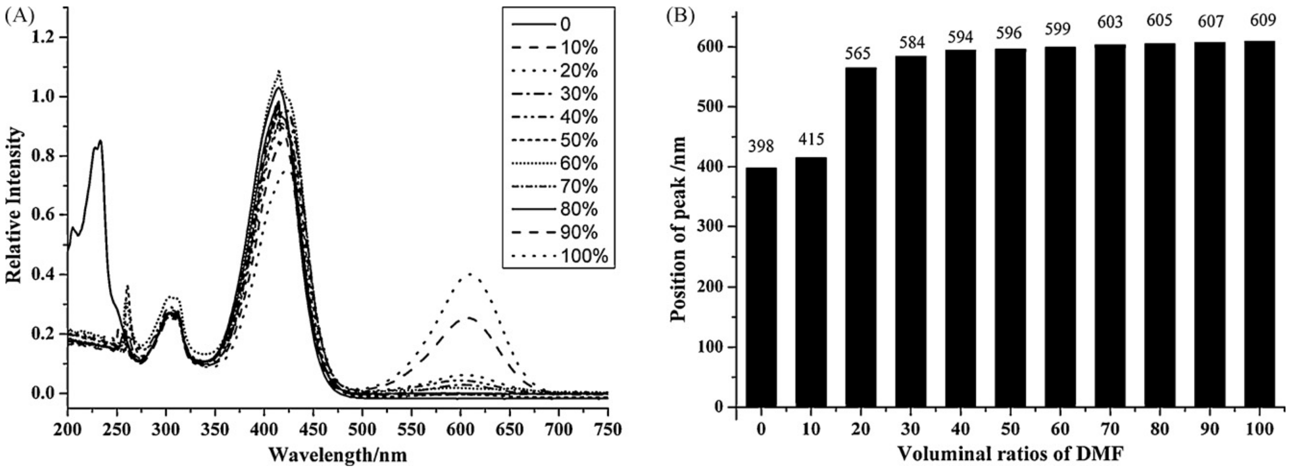

**Fig. 8.** UV–vis spectra of DAFND in mixed solvents and the positions of the maximal absorption peak.

**Table 4**
Solvatochromic data for DAFPD and DAFND in various liquid solvents.

| Solvent | DAFPD | | DAFND | | $\pi^*$ | $\alpha$ | $\beta$ |
|---|---|---|---|---|---|---|---|
| | $\lambda_{max}$ (nm) | $\upsilon_{max}$ $\times 10^3$ ($cm^{-1}$) | $\lambda_{max}$ (nm) | $\upsilon_{max}$ $\times 10^3$ ($cm^{-1}$) | | | |
| Py | 395 | 25.32 | 614 | 16.27 | 87 | 00 | 64 |
| DMSO | 396 | 25.25 | 613 | 16.31 | 100 | 00 | 76 |
| Glycol | 395 | 25.32 | 610 | 16.40 | 92 | 90 | 52 |
| DMF | 395 | 25.32 | 609 | 16.42 | 88 | 00 | 69 |
| $CH_3CN$ | 394 | 25.38 | 597 | 16.75 | 75 | 19 | 40 |
| $C_2H_5OH$ | 395 | 25.32 | 430 | 23.26 | 54 | 86 | 75 |
| THF | 394 | 25.38 | 429 | 23.31 | 58 | 00 | 55 |
| $(CH_3)_2CO$ | 393 | 25.44 | 428 | 23.36 | 71 | 08 | 43 |
| $CH_3OH$ | 395 | 25.32 | 425 | 23.53 | 60 | 98 | 66 |
| Isoamylol | 395 | 25.32 | 423 | 23.64 | 40 | 84 | 86 |
| Isopropanol | 394 | 25.38 | 423 | 23.64 | 48 | 76 | 84 |
| Ethyl acetate | 396 | 25.25 | 418 | 23.92 | 55 | 00 | 45 |
| Dioxane | 396 | 25.25 | 417 | 23.98 | 55 | 00 | 37 |
| $CHCl_3$ | 395 | 25.32 | 414 | 24.15 | 58 | 20 | 10 |
| $CH_2Cl_2$ | 395 | 25.32 | 413 | 24.21 | 82 | 13 | 10 |
| $H_2O$ | – | – | 392 | 25.51 | 109 | 117 | 47 |
| $C_6H_5CH_3$ | 395 | 25.32 | 370 | 27.03 | 54 | 00 | 11 |

DMF: N,N′-dimethylformamide, DMSO: dimethylsulfoxide, Py: pyridine, THF: tetrahydrofuran.

contributions. $E_0$ is the transition energy for a solvent where $\pi^* = \alpha = \beta = 0$ (e.g. cyclohexane).

The individual form of the LSER for DAFND is given by Eq. (2) based on the data in Table 4, Eq. (1) and published values of $\pi^*$, $\alpha$ and $\beta$ [30]

$$E = 35.03 - 19.66\pi * -0.1543\alpha - 0.0008\beta \quad (2)$$

where energy units are $10^3$ $cm^{-1}$ (kK), and $n = 16$ (the data of $H_2O$ are omitted), $r = 0.965$, SD = 513 $cm^{-1}$. Points to be emphasized are as follows:

(1) The value for $E_0$ corresponds to a transition absorption maximum of 285 nm, which is well consistent with the polarity order (cyclohexane 0.1 is lower than toluene 2.4).
(2) The coefficient for $\pi^*$ and $\beta$ are much more larger and smaller than those of the other compounds [29,31–33], indicating DAFND hold unusual solvatochromism for example the obvious difference of $\lambda_{max}$ in various solvents. $\lambda_{max}$ in polar solvent is notably larger than that of nonpolar or low polar solvent shown in Table 4, which is also demonstrated by the $\lambda_{max}$ in the mixed solvents of methanol and DMF with different ratios shown in Fig. 8.

## 4. Conclusions

A novel Schiff base of 4,5-diazafluorene-9-*p*-nitrophenylhydrazone was synthesized. X-ray analyses reveal that the planarity of DAFND is better than that of 4,5-diazafluorene-9-phenylhydrazone in solid state and the nitro group affects the planarity of the compound and crystal structures. The UV–vis spectra investigation exhibits that DAFND has thermochromism and solvatochromism determined by the nitro group. The color of DAFND changes from brown to green and blue at about 95 °C in solid state, furthermore, the colors of DAFND are diverse in different pure solvents at the same conditions.

## Acknowledgments

This work is financially support by the National Natural Science Foundation of China (60877048) and the Program for Changjiang Scholars and Innovative Research Team in University (IRT0547), Ministry of Education, China.

## Appendix A. Supplementary data

Supplementary data associated with this article can be found, in the online version, at doi:10.1016/j.saa.2009.11.050.

## References

[1] A.A. Salem, Y.M. Issa, M.I. Ayad, M. Elkholy, J. Mater. Sci.: Mater. Electron. 5 (1994) 199–202.
[2] L. Burgio, P.J. Gibbs, Spectrochim. Acta A 57 (2001) 1491–1521.
[3] W. Strunk Jr., E.B. White, The Elements of Style, third ed., Macmillan, New York, 1979.
[4] G.R. Mettam, L.B. Adams, in: B.S. Jones, R.Z. Smith (Eds.), Introduction to the Electronic Age, E-Publishing, Inc., New York, 1994, pp. 281–304.
[5] D.K. Johnson, T.B. Murphy, N.J. Rose, W.H. Goodwin, L. Pickart, J. Inorg. Chim. Acta 67 (1982) 159–165.
[6] B.E. Love, E.G. Jones, J. Org. Chem. 64 (1999) 3755–3756.
[7] G. Yang, J.Z. Wu, L. Wang, T.X. Zeng, L.N. Ji, X. Tian, J. Inorg. Biochem. 66 (1997) 141–144.
[8] J. Albert, A. Gonzalez, J. Granell, R. Moragas, C. Puerta, P. Valerga, Organometallics 16 (1997) 3775–3778.
[9] J.H. Day, Chem. Rev. 63 (1963) 65–80.
[10] A. Samat, V. Lokshin, in: J.C. Crano, R.J. Guglielmetti (Eds.), Organic Photochromic and Thermochromic Compounds, Kluwer Academic/Plenum Publishers, New York, 1999.
[11] C. Reichardt, Solvent Effects in Organic Chemistry, 2nd ed., Wiley-VCH, Weinheim, 1988.
[12] V.C. Fernández, I.R. Matías, F.J. Arregui, R.D. Joaquin, A.V. Jose, M. Jimenez, Opt. Eng. 42 (2003) 656–661.
[13] M.A. White, M. LeBlanc, J. Chem. Educ. 76 (1999) 1201–1205.
[14] D. Laage, W.H. Thompson, M. Blanchard-Desce, J.T. Hynes, J. Phys. Chem. A 107 (2003) 6032–6046.
[15] T.A. Fayed, Colloids Surf. A 236 (2004) 171–177.
[16] X. Yang, W.H. Liu, W.J. Jin, G.L. Shen, R.Q. Yu, Spectrochim. Acta, Part A 55 (1999) 2719–2727.
[17] J. Mlochowski, Z. Szulc, Polish J. Chem. 57 (1983) 33–39.
[18] L.J. Henderson, J.F.R. Fronczek, W.R. Cherry, J. Am. Chem. Soc. 106 (1984) 5876–5879.
[19] G.M. Sheldrick, SADABS: Program for Empirical Absorption Correction of Area Detector Data, University of Göttingen, Germany, 1996.
[20] G.M. Sheldrick, SHELXL97, Program for Crystal Structure Refinement, University of Göttingen, Germany, 1997.
[21] A.L. Spek, Acta Crystallogr. Sect. A46 (1990) C34.
[22] G. Yang, J.Z. Wu, L. Wang, T.X. Zeng, L.N. Ji, Acta Sci. Nat. Univ. Sunyatseni 1 (1997) 45–47.
[23] T. Tunc, H. Tezcan, M. Sari, O. Büyükgüngör, R. Yagbasan, Acta Cryst. C59 (2003) o528–o529.
[24] C.L. Jones, G.H. Milburn, L. Sayer, D.L. Hughes, Acta Cryst. B37 (1981) 1548–1553.
[25] G.G. Evans, J.A. Boeyens, Acta Cryst. B45 (1989) 581–590.
[26] T. Inabe, N. Hoshino, T. Mitani, Y. Maruyama, Bull. Chem. Soc. Jpn. 62 (1989) 2245–2251.
[27] E. Hadjoudis, I.M. Mavridis, Chem. Soc. Rev. 33 (2004) 579–588.
[28] E. Buncel, S. Rajagopal, Acc. Chem. Res. 23 (1990) 226–231.
[29] M.J. Kamlet, J.L.M. Abboud, R.W. Taft, Prog. Phys. Org. Chem. 13 (1981) 485–630.
[30] Y. Marcus, Chem. Soc. Rev. 94 (1993) 409–416.
[31] A.A. Gorman, M.G. Hutchings, P.D. Wood, J. Am. Chem. Soc. 118 (1996) 8497–8498.
[32] I. Bolz, C. May, S. Spange, New J. Chem. 31 (2007) 1568–1571.
[33] K. Dimroth, C. Reichardt, T. Siepmann, F. Bohlmann, Liebigs Ann. Chem. 661 (1963) 1–37.